IEIE Transactions on Smart Processing and Computing, vol. 4, no. 5, October 2015
http://dx.doi.org/10.5573/IEIESPC.2015.4.5.324

IEIE Transactions on Smart Processing and Computing

Development of SiPM-based Small-animal PET

Jin Hyung Lee, Seung-Jae Lee, and Yong Hyun Chung*

Department of Radiological Science, College of Health Science, Yonsei University / Wonju, Republic of Korea
Jinhyung1@naver.com, n-esses21@nate.com, ychung@yonsei.ac.kr

***** Corresponding Author: Yong Hyun Chung

Received October 15, 2015; Revised October 21, 2015; Accepted October 25, 2015; Published October 31, 2015

** Regular Paper*

Abstract**:** A decreased number of readout method is investigated to provide precise pixel information for small-animal positron emission tomography (PET). Small-animal PET consists of eight modules, and each module is composed of a 6 × 6 array of 2 × 2 × 20 mm^3 lutetium yttrium orthosilicate (LYSO) crystals optically coupled to a 4 × 4 array of 3 × 3 mm^2 silicon photomultipliers (SiPMs). The number of readout channels is reduced by one-quarter that of the conventional method by applying a simplified row and column matrix algorithm. The performance of the PET system and detector module was evaluated with Geant4 Application for Emission Tomography (GATE) 6.1 and DETECT2000 simulations. In the results, all pixels of the 6 × 6 LYSO array were decoded well, and the spatial resolution and sensitivity, respectively, of the PET system were 1.75 mm and 4.6% (@ center of field of view, energy window: 350-650 keV).

Keywords**:** SiPM, Small-animal PET, Algorithm, GATE simulation, DETECT2000 simulation

1. Introduction

The onset of disease usually brings functional and/or biochemical changes in an organ or tissue before anatomic changes. Recently, research into molecular imaging has been progressing rapidly for early diagnosis of initial changes in a lesion. In molecular imaging, positron emission tomography (PET) is an analytical imaging technique that provides a way of making in vivo measurements of anatomic distribution and biochemical changes. PET detects pairs of gamma rays emitted indirectly by a positron emitting radionuclide (or tracer), which is administrated into the body on a biologically active molecule. So, small animal research, which is widely used in laboratories for biomedical research, drug and vaccine development, gene expression and novel detector technology, is an emerging field in preclinical molecular imaging with PET in nuclear medicine [1]. Small-animal PET has a compact size suitable for small animals like mice, rats, rabbits and primates, and offers improved sensitivity and resolution, compared with clinical PET.

The image acquisition process for PET is as follows. First, positron emitting isotopes, such as F-18 and O-15, are injected into specified locations. The emitted positrons annihilate nearby electrons, emitting two 511 keV photons, directed 180 degrees apart. These photons are then detected by the scanner, which can estimate the density of positron annihilations in a specific area [2]. To easily detect two gamma rays in opposite directions, the geometry of the prevalent PET system is a circular arrangement of detector modules. Each detector module consists of several arrays of sub-modules, as shown in Fig. 1.

Fig. 2 shows schematic diagrams of three types of PET detector. Currently, PET systems in the medical imaging market are mostly based on a photomultiplier tube (PMT) light collection system [3-6]. This method is based on Anger logic calculating the position of interacted pixels using weighted X+, X-, Y+, and Y- signals [7]. However, a detector module using PMT is bulky, and the flood histogram generated using Anger logic shows a well-known pincushion distorted shape.

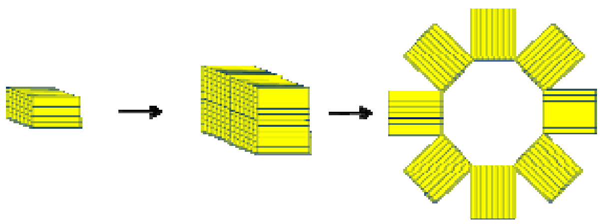

Fig. 1. PET system composed of sub-modules.

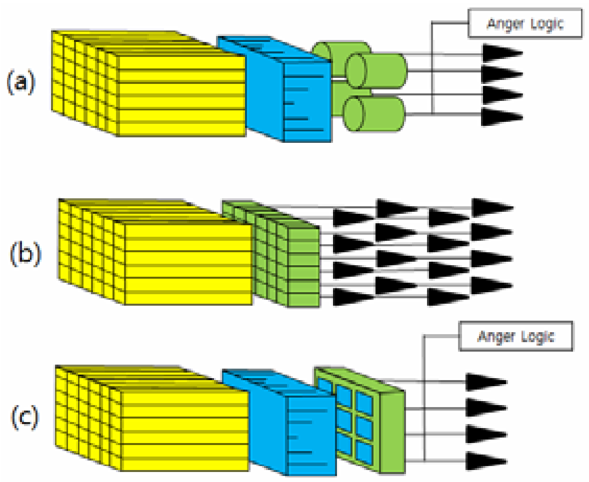

Fig. 2. The schema of conventional small-animal PET detector sub-modules: (a) PMT-based, (b) one-to-one matched, and (c) many-to-one matched modules.

Table 1. Experiment Parameters.

Detector	PMT	APD	SiPM
Quantum Efficiency (@ 420 nm) [%]	<40	<70	<80
Single Photon Resolution	○	×	○
Operation Voltage [V]	1000 – 3000	1000 – 2000	10 – 100
Gain	~ 10^6	~ 10^2	~ 10^6
Insensitivity to Magnetic Field	×	○	○
Miniaturization	×	○	○
Production Costs	Medium	Low	Potentially Low

To overcome the disadvantages of a PMT-based system, many research teams applied other photodetectors, such as the avalanche photodiode (APD) and the silicon photomultiplier (SiPM). Above all, SiPM has advantages in quantum efficiency, operation voltage, gain, and simple data readout methods, compared to other detectors [8], and Table 1 shows detailed specifications of photodetectors that can be used for PET systems [2, 9].

A small animal PET system using a SiPM detector has been actively discussed and studied by many research facilities. In the initial stages of SiPM-based PET studies, a one-to-one (crystal-to-SiPM) matched detector was considered in which the number of pixelated crystals and SiPMs sensors is the same, and the pixel position is digitized directly without Anger logic. The drawback of this detector is the large number of data channels in the electronics.

As an alternate method, a many-to-one (crystal-to-SiPM) matching detector was discussed and studied [10]. Compared to the one-to-one matched detector, the many-to-one matched method employed a reduced number of SiPMs by using a light guide and Anger logic. It has the advantages of low cost with a small number of SiPMs and data channels in the electronics, but it suffers from image distortion via Anger logic.

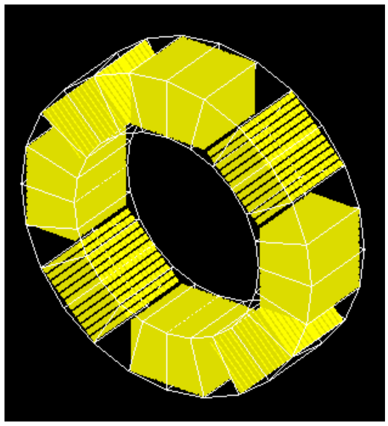

Fig. 3. GATE simulated geometry of a PET scanner

In order to overcome the flaws in the existing techniques (e.g. The high cost of a PET system, complicated data readout and acquisition systems), we designed a modified many-to-one (crystal-to-SiPM) matched detector for small-animal PET. In this detector, a position determination algorithm was implemented for pixel positioning instead of Anger logic. To evaluate the performance of the proposed detector and PET system, Monte Carlo simulation studies were performed using Geant4 Application for Emission Tomography (GATE), a simulation toolkit for PET and single photon emission computed tomography (SPECT) [11], and DETECT2000, a Monte Carlo code for light photon transport [12].

2. Materials and Methods

2.1 Design of PET System and Position Determination Algorithm

The PET system consists of eight modules arranged in a circular shape with a diameter of 76 mm. A single module contains a 2 × 2 array of sub-modules composed of 6 × 6 lutetium yttrium orthosilicate (LYSO) scintillators directly coupled to a 4 × 4 SiPM array. Each LYSO is 2.0 × 2.0 × 20.0 mm^3, and a SiPM has a 3.0 × 3.0 mm^2 area. Fig. 3 shows the GATE simulated geometry of the PET scanner. A total of 1,152 LYSO pixels, 512 SiPMs and 256 Analog to Digital Converter (ADC) channels are required.

The 4 × 4 SiPM signals of a single gamma event are multiplexed into 4 X and 4 Y channels as shown in Fig. 4 and recorded in list mode. Then, X and Y positions of LYSO pixels are directly digitized by using a position determination algorithm. Eight channels of each event data are saved in a two-dimensional matrix, Data (i, j) where i = 1,2,…,8, and j = 1,2,…, count, and the energy of the event is calculated for energy discrimination as follows:

$$\text{Energy}(j) = \sum_{i=1}^{8} \frac{\text{Data}(i,j)}{2} \qquad (1)$$

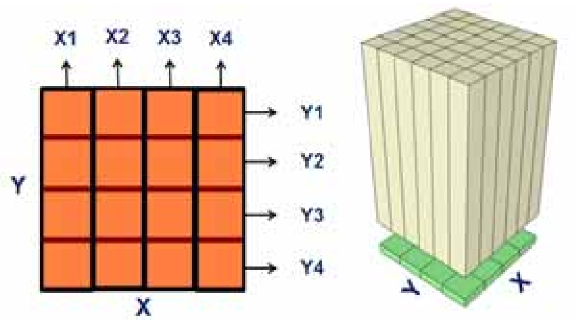

Fig. 4. Illustration of a sub-module and the eight-channel multiplexing readout .

If the energy falls within the preselected energy window, it passes to the pixel positioning process. To find the X and Y positions of the event, the mean of eight channels is obtained by

$$\text{Mean (j)} = \sum_{i=1}^{8} \frac{Data\left(i,\, j\right)}{8} \tag{2}$$

When the i-th channel signal of the j-th event is larger than the mean value, 1 is written in POS (i,j) otherwise, 0 is written. Eight digitized numbers in the POS (i,j) array represent eight channels. For example, POS(i) equal to a {1, 0, 0, 0, 1, 0, 0, 0} array shows that the number of detected light photons in X1 and Y1 channels is greater than the mean value. Therefore, the combination of X1 and Y1 channels is represented with the first pixel of the crystal array. Then, the final pixel number is determined using eight digitized numbers. The flow chart of the position determination algorithm is shown in Fig. 5.

2.2 GATE Simulation

To evaluate the performance of the proposed PET scanner, the PET system was modeled and simulated through GATE v6.1. System sensitivity was simulated using a 10 MBq point source, and the source position was moved in 5 mm steps from the center of the scanner in radial and axial directions. Three different energy windows were used: 250 – 650, 350 – 650 and 450 – 650 keV. The spatial resolution at the center was also calculated with an energy window of 350 – 650 keV.

2.3 DETECT2000 Simulation

Light photon distribution within the scintillation crystal is the main concern for developing the position determination algorithm. The light distribution in the detector was modeled by the Monte Carlo–based simulation tool, DETECT2000. The proposed sub-module was modeled as a 6 × 6 LYSO array with a pixel size of 2.0 × 2.0 × 20.0 mm^3. The inter-crystal reflectors are 3M enhanced specular reflector film (0.065mm thickness). The crystal array was optically coupled to a 4 × 4 SiPM array with 0.2 mm gap between SiPMs. The refractive indices of LYSO and the optical grease were set to 1.82 and 1.465, respectively.

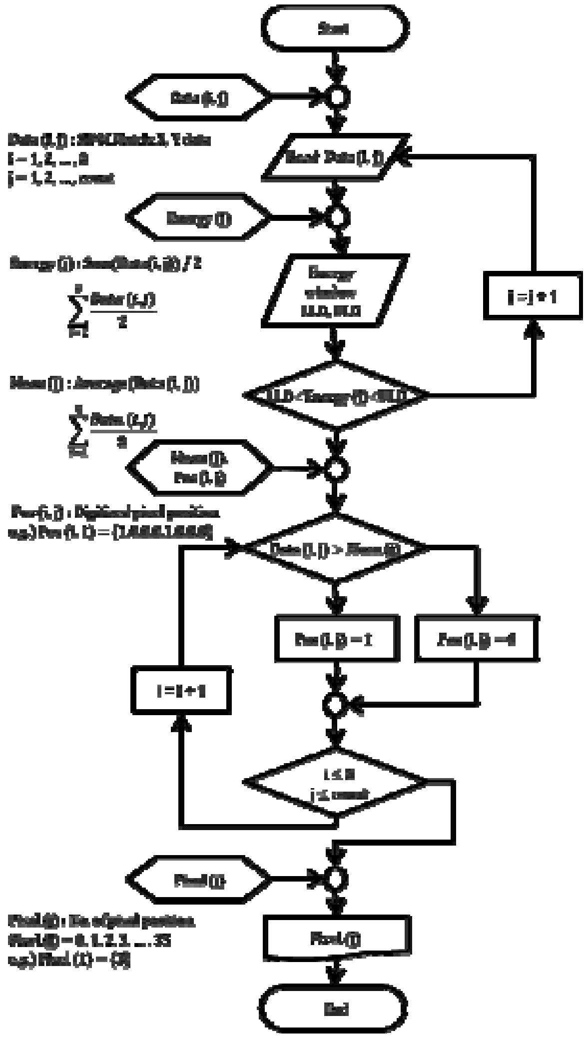

Fig. 5. Flow chart of the position determination algorithm.

The thickness of the optical grease was defined as 0.01 mm. In each gamma event, a total of 4,800 light photons were generated, considering the light yield of LYSO and the quantum efficiency of SiPM. One thousand gamma events were generated in each pixel, and the capability of pixel positioning by the proposed algorithm was evaluated.

3. Results

3.1 Spatial Resolution of PET System

Fig. 6(a) shows the sinogram and image of a 10 MBq point source at the center of the scanner reconstructed by a filtered back projection (FBP) algorithm. Fig. 6(b) illustrates the radial profile and Gaussian fitted curve. The measured FWHM was 1.741 mm and 1.760 mm in radial and tangential directions, respectively.

3.2 Sensitivity

The source was moved along the central axis of the scanner to record the number of coincidences acquired as a function of the source location. The ratio between the

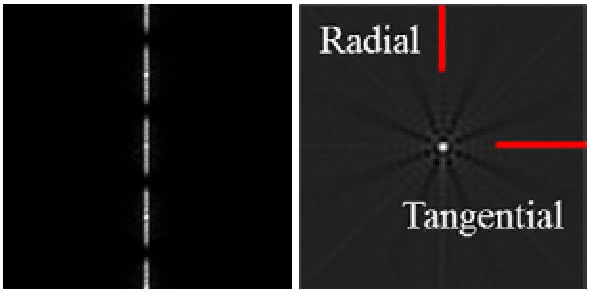

(a)

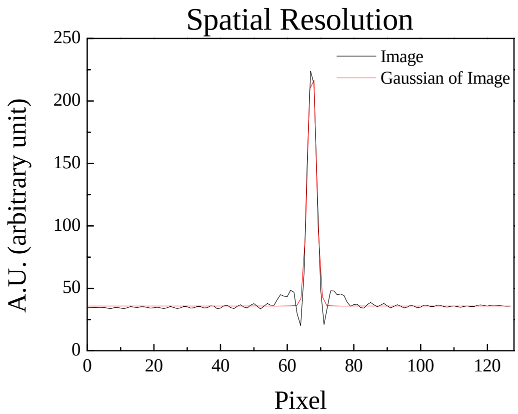

(b)

Fig. 6. (a) Sinogram and image of a 10 MBq point source; (b) radial profile and Gaussian fitted curve.

Table 2. Sensitivity @ center.

Energy Window [keV]		
250 - 650	350 - 650	450 - 650
5.34%	**4.59%**	**3.30%**

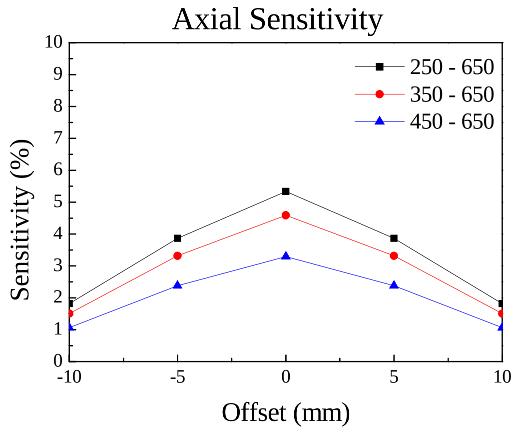

(a)

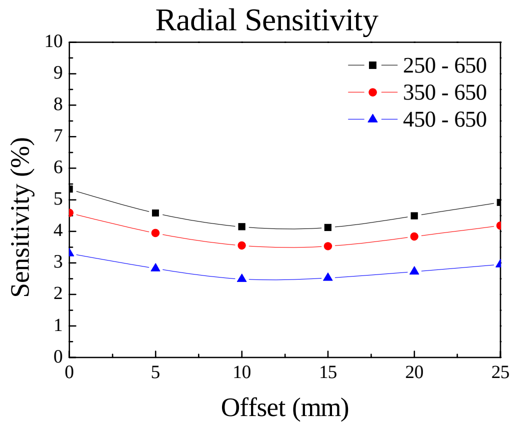

(b)

Fig. 7. System sensitivity as a function of the source location along (a) the axial direction and (b) the radial direction.

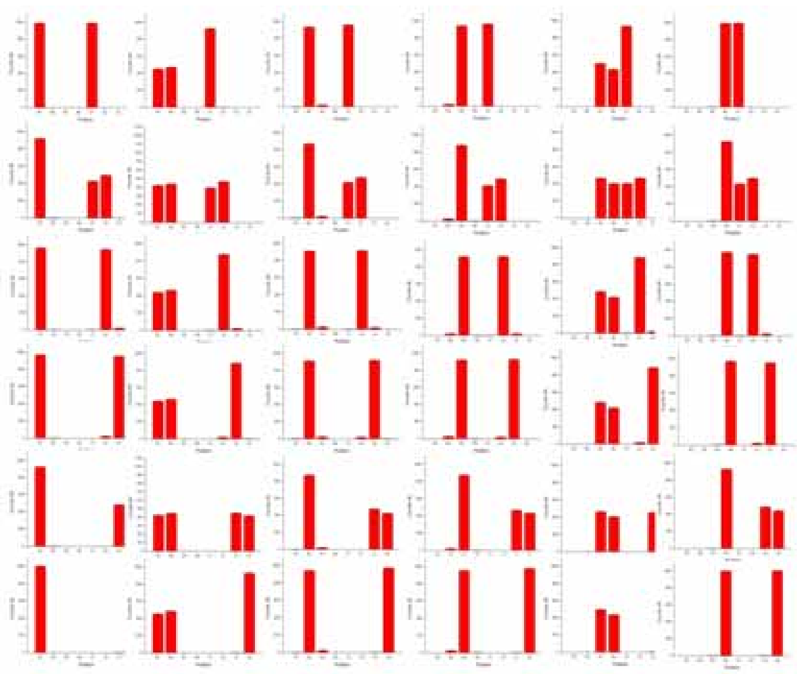

Fig. 8. Eight channel signals of the 6 × 6 crystal array when the gamma event was detected in each pixel.

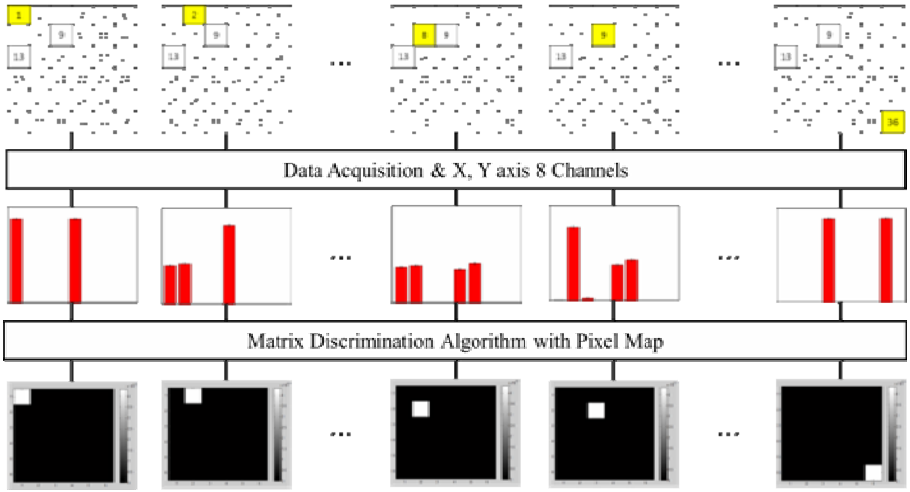

Fig. 9. Schematic diagram of the pixel positioning pro-cedure.

Table 3. Comparison of the PET performances

Sensitivity @ center [%]	Module [mm^3]	Radial / Axial FOV [mm]	Spatial resolution @ center [mm]	Photon Sensitivity [%]	Remark
Siemens Inveon	1.6 × 1.6 × 10 LYSO	161 / 127	1.4 with FBP	≥ 10	PSPMT, Optical fiber
PerkinElmer G8 PET/CT	1.75 × 1.75 × 7.2 BGO	47 / 95	1.4 with 3D ML-EM	> 14	Avalanche Photo Diode
Mediso NanoScan	1.51 × 1.51 × 10 LYSO	80 / 100	1.4 with FBP 0.9 with 3D OSEM	7	512Ch/Module APD
Proposed PET system	2.0 × 2.0 × 20 LYSO	76 / 31	1.75 with FBP	4.6	256Ch ADC, SiPM

recoded coincidence counting rate and the source activity provided the system sensitivity as a function of the source location along the axial and radial directions, shown in Figs. 7(a) and (b), respectively. The difference in sensitivity was also evaluated by applying three different energy windows, as summarized in Table 2.

3.3 Pixel Identification

Fig. 8 demonstrates the eight channel signals of the 6 × 6 crystal array acquired from the gamma event arising in each crystal pixel. The schematic diagram of the pixel identification and image acquisition procedure is illustrated in Fig. 9. It indicates that all pixels were decoded well by the proposed position determination algorithm.

4. Discussion and Conclusion

In this study, a small-animal PET system using SiPM photo sensors was designed employing a many-to-one (crystal-to-SiPM) matched detector sub-module, and its performance was evaluated through Monte Carlo simulations. The number of readout channels can be reduced in this design while system performance is maintained. In the results, all pixels of the 6 × 6 sub-module array were decoded well, and the spatial resolution and sensitivity of the PET system were estimated as 1.75 mm FWHM and 4.6% (@ center of field of view, energy window 350 - 650 keV), respectively.

The performances of the proposed PET system and of commercially available small-animal PET systems are shown in Table 3.

Acknowledgement

This work was supported by the BK21 Plus program through the National Research Foundation (NRF) funded by the Ministry of Education of Korea

References

[1] R. Yao et al., "Small-animal PET: what is it, and why do we need it?," *J. Nucl. Med. Techno*, Vol. 40, pp. 157-165, May 2012. Article (CrossRefLink)

[2] S. R. Cherry et al., Physics in Nuclear Medicine 3rd ed. (Saunders), 2003

[3] S. R. Cherry et al., "MicroPET: a high resolution PET scanner for imaging small animals," *IEEE*

Trans. Nucl. Sci. Vol. 44, no. 3, pp. 1161-1166, Jun 1997. Article (CrossRefLink)
[4] Y. Wang et al., "Performance evaluation of the GE Healthcare eXplore VISTA dual-ring small-animal PET scanner," *J. Nucl. Med*. Vol. 47, no. 11, pp. 1891-1900, November 2006. Article (CrossRef Link)
[5] S. Surti et al., "Design evaluation of A-PET: a high sensitivity animal PET camera," *IEEE Trans.Nucl. Sci*. Vol. 50, no. 5, pp. 1357-1363, October 2003. Article (CrossRef Link)
[6] K. Ziemonsa et al., "The ClearPET^{TM} project: development of a 2nd generation high-performance small animal PET scanner," *Nucl. Instrum. Methods Phys. Res. A* Vol. 537, no. 1-2, pp. 307-311, January 2005. Article (CrossRef Link)
[7] H.O. Anger et al., "Scintillation camera" *Rev. Sci. Instrum.* 29, 27, 1958. Article (CrossRef Link)
[8] E. Roncali et al., "Application of silicon photo-multipliers to positron emission tomography," *Annals of Biomedical Engineering*, Vol. 39, No. 4, pp. 1358−1377, April 2011. Article (CrossRef Link)
[9] KETEK SIPM TECHNOLOGY. Available at: Article (CrossRef Link)
[10] M. Ito et al., "Design and simulation of a novel method for determining depth-of-interaction in a PET scintillation crystal array using a single-ended readout by a multi-anode PMT," *Nucl. Instrum. Methods Phys. Res. A* Vol. 743, pp. 30-38, 2014. Article (CrossRef Link)
[11] S. Jan et al., "GATE: a simulation toolkit for PET and SPECT," *Phys. Med. Biol*. Vol. 49, pp. 4543-4561, September 2004. Article (CrossRef Link)
[12] F. Cayouette et al., "DETECT2000: Monte-Carlo simulator for the computer aided design of photon sensing devices," *SPIE* 4833, Applications of Photonic Technology 5, 69, February 2003. Article (CrossRef Link)

Jin Hyung Lee received a BSc from the department of radiological science at Yonsei University, Republic of Korea, in 2014. He is currently pursuing his master's degree in the molecular imaging laboratory, Yonsei University. His current research topics include Monte Carlo simulations for medical imaging device modeling.

Seung-Jae Lee received an MSc from the department of radiological science at Yonsei University, Republic of Korea. He is in the ongoing doctoral program in the molecular imaging laboratory, Yonsei University. His current research topics include Monte Carlo simulations for medical imaging device modeling.

Yong Hyun Chung has been a Professor in the Department of Radiation Convergence Engineering at Yonsei University since 2006. He received his BSc, MSc, and PhD from the Department of Nuclear and Quantum Engineering at KAIST, South Korea, and majored in radiation detection and medical imaging, especially for nuclear medicine instrumentation. From 2002 to 2006, he worked as a Researcher in the Department of Nuclear Medicine, Samsung Medical Center, Seoul, Korea, at the Center for Clinical Research, Samsung Biomedical Research Institute, Seoul, Korea, and at the Crump Institute for Molecular Imaging, David Geffen School of Medicine, UCLA, Los Angeles, USA. His current interests lie in the area of non-invasive imaging techniques, like gamma cameras, single photon emission computed tomography (SPECT), positron emission tomography (PET), and specific nuclear material (SNM) monitoring systems.